

## Introduction

Initial preparation of specific electronic state can dictate the following dynamics, which often precedes on several, coupled potential energy surfaces (PES) for example, fast transition to another electronic state which leads to nuclear motion to form a new geometrical structure of the molecule. Such processes are of a big interest, while a basic example for coupling between nuclear and electronic motion is Jahn-Teller (J-T) theorem.<sup>1</sup> Classic examples of molecules which suffer such a J-T distortion is a benzene cation ( $Bz^+$ ).

By taking into advantage the remarkable sensitivity of soft X-ray transient absorption spectroscopy from the core level in the carbon 1s K-edge to different molecular orbitals, it is possible to distinguish between different molecular structure related to different electronic states of neutral molecules and positive ions with sensitivity to local carbon atoms.<sup>2,3,4</sup> While the ability to probe positive ions open a new experimental opportunity which is not accessible with common techniques. Among many different predicted and partly observed dynamics of the prepared cation, benzene and halogenated benzene molecules catch a big interest, where number of fundamental questions about these molecules will be answered in this work, in particularly benzene ( $Bz$ ) and bromobenzene ( $BrBz$ ).

In the neutral ground state of the benzene molecule the  $\pi$  electronic configuration is  $(a_{2u})^2(e_{1g})^4$ , while in benzene cation this configuration change. By removing one electron from a degenerate bonding  $e_{1g}$  orbital, which is highest occupied molecular orbital, (HOMO) positive benzene ion prepared ( $Bz^+$ ). As a result, the energetic degeneracy of  $e_{2g}$  orbitals removed by J-T distortion, and giving rise to the two different electronic states,  $^2B_{2g}$ , with unpaired electron occupies the  $b_{2g}$  orbital and two electrons in  $b_{1g}$ . Or,  $^2B_{1g}$  electronic state with unpaired electron occupies the  $b_{1g}$  orbital and two electrons in  $b_{2g}$  orbital. The electronic splitting cause to two different geometries structure of  $Bz^+$  ( $D_{2h}$  symmetry), in contrast to  $Bz$  ( $D_{6h}$  symmetry),<sup>5</sup> where the geometric structure of benzene ring is a hexagonal with same C-C bond length of 1.400 Å, the prepared  $Bz^+$  in  $^2B_{2g}$  electronic state has compressed hexagonal structure of the benzene ring, the  $C_2-C_3$  and  $C_5-C_6$  bond length calculated to be 1.377 Å while the other C-C bonds are 1.431 Å. For  $Bz^+$  prepared in  $^2B_{1g}$  electronic state, benzene ring has elongated forms with calculated  $C_2-C_3$  and  $C_5-C_6$  bond length to be 1.454 Å while the other C-C bonds are 1.389 Å.<sup>6</sup>

The nature of the distorted structures can be qualitatively understood within  $D_{2h}$  symmetry. The  ${}^2B_{2g}$  state has two electrons in the  $b_{1g}$  orbital and one electron in the  $b_{2g}$  orbital. Since the  $b_{1g}$  orbital is anti-bonding (changes sign from positive to negative at a nodal plane between two atoms) between  $C_2$  and  $C_3$  and between  $C_5$  and  $C_6$ , an elongated  $D_{2h}$  structure is adopted by this configuration. Similarly the  ${}^2B_{2g}$  state adopts a compressed  $D_{2h}$  structure because  $b_{2g}$  has more electron density between the two nuclei,  $C_2$  and  $C_3$  and between  $C_5$  and  $C_6$ . From recent calculations, the energy difference between compressed and elongated  $Bz^+$  showed a similar trend of about 0.10 - 2.33 kcal/mol, where the compressed  $Bz^+$  is more stable.<sup>7</sup> The heights of the activation barriers, the energy difference between  $Bz^+$  at the vertical ionization point from parent neutral benzene and energy of the compressed form were calculated to be 3.5 kcal/mol.<sup>7</sup> The splitting of the electronic state to the compressed and elongated forms happens almost simultaneously, both of the forms calculated to reach their average bond length values in the time range 10–12 fs,<sup>7</sup> and therefore very hard to be observed in the time domain experiments. Experimentally, J-T distortion in  $Bz^+$  mostly observed from vibrational spectroscopic interpretation.

However, by substitution halogen atom (Cl, Br, F, I) with hydrogen the degenerated orbitals  $e_{2g}$  split to  $1a_2$  and  $3b_1$  orbitals (in  $C_{2v}$  symmetry) in the neutral  $XBz$  ( $X = Cl, Br, F, I$ ).  $1a_2$  shows almost pure benzenoid character with very similar electron distribution to  $b_{2g}$ .  $3b_1$ , the highest occupied molecular orbital (HOMO) has strong  $\pi$ -electron ring mixing with the halogen atom and similar electron distribution on the benzene ring to  $b_{1g}$ . The ionization processes of these molecules correspond to loss of a single electron from each of the HOMO  $3b_1$  and HOMO-1  $1a_2$ , lead to two lowest ionic states of  $X-Bz^+$ ,  $X^2B_1$  and  $A^2A_2$  corresponded to compressed and elongated forms of the benzene ring respectively, very similar to  ${}^2B_{2g}$  and  ${}^2B_{1g}$  in  $Bz^+$ . The energy difference between the split orbitals are 0.54, 0.6, 0.66 and 0.7 eV for IBz, ClBz, BrBz and FBz respectively.<sup>8,9,10,11</sup> Due to the electronic distribution and geometry form similar to the two lowest ionic states in  $XBz$  compare to the splitted states by JT distortion in  $Bz^+$  a strong coupling expected also in these types of molecules. Indeed, ab initio calculation revealed CI between  $3b_1^{-1}$  and  $1a_2^{-1}$  in  $FBz^+$ ,<sup>12</sup> with two strong coupling vibrational modes,  $\nu_6$  (618  $cm^{-1}$ ) and  $\nu_{25}$  (1638  $cm^{-1}$ ) of  $B_2$  symmetry. In addition, similar mechanism was found for three higher ionization states,<sup>12</sup> and later on weak coupling was found between these two groups,<sup>13</sup> which gave reasonable explanation to absence of fluorescence from these ionic states. Later

on, theoretically calculations of  $\text{FBz}^+$  considering several CIs among lowest five electronic surfaces using TDDVR approach,<sup>14</sup> shows reasonably good agreement with previous calculations.<sup>12,13</sup> recently several works on  $\text{ClBz}^+$ ,  $\text{BrBz}^+$ , and  $\text{FBz}^+$  show from vibrational spectroscopy analysis experimental evidence for vibronic coupling between electronic states.<sup>9,10,11</sup> The potential surface in this region was calculated for  $\text{FBz}^+$  and the CI between  $X^2B_1$  and  $A^2A_2$  was observed from that calculations. (See figure 1)

With two photons of 266 nm it is possible to ionized ClBz and BrBz by resonantly enhanced multiphoton ionization (REMPI) only from HOMO, it means, the lowest specific electronic state of the positive ion is well define unlike in  $\text{Bz}^+$ .  
●Therefore, with our ~100 fs system temporal resolution it may be possible to observe experimental evidence for the passage from  $X^2B_1$  to  $A^2A_2$  state. ●Moreover, by great sensitivity to different electronic states it may be possible to observe these two states spectrally separated in transient absorption spectrum in the carbon k-edge region.

In addition, it is of great interest to observe partly occupied  $\pi$  orbital of the cation or of neutral excited ( $\pi \rightarrow \pi^*$ ) molecule, and to figure out if the transition probability from different carbons will change due to ionization or excitation. ●In particular, excitation from the core level of the carbons bonded to hydrogen atom compare to the carbon bonded to bromine atom. ●Moreover, by comparing excited neutral BrBz spectrum with  $\text{BrBz}^+$  it may be possible to conclude about basic principle of transition to unoccupied or partly occupied orbitals.

●It is well known that initial vibrational excitation can change drastically transition probability to excited electronic state due to FC factor. In this contest, it will be interesting to observe how different prepared vibrational states influence on the transition from the core level. Ionization with (1+1) REMPI bring us to different vibrational states compare to cation ground state which slightly shifted between  $\text{BrBz}^+$  and  $\text{ClBz}^+$  molecules, and therefore the responds to x-ray may be different, especially based on previous study that show a great depends of x-ray spectra on vibrational transitions.<sup>15</sup>

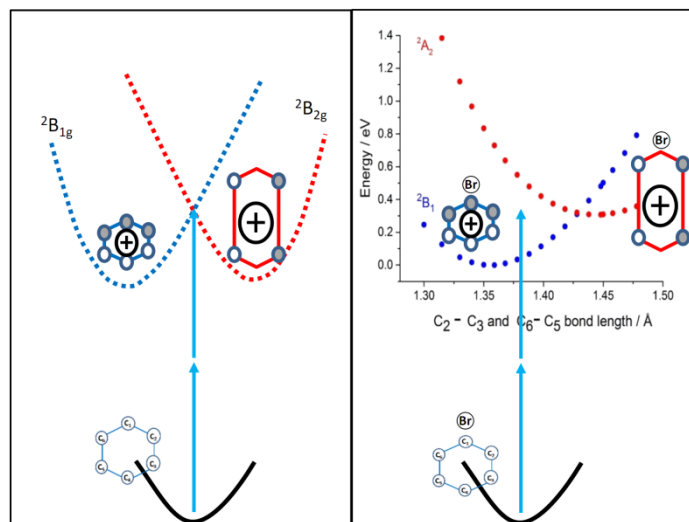


**Figure 1.** Schematic potential energy curves of Jahn-Teller distortion of a benzene cation (left), as a result of (1+1) REMPI, and expected potential energy curves of bromobenzene cation (right). The presented potential curve on the right side is calculated energy profile of fluorobenzene cation taken from supplementary material of ref 11.

## Methods

The key components of the experimental setup to produce soft x-ray static absorption spectrum and UV-pump, soft x-ray probe transient absorption spectrum includes a detection apparatus and a laser system (Spectra-Physics, Spitfire-ACE-PA) delivers 12 mJ pulses at 1 kHz repetition rate, 35 fs pulse duration, with a wavelength centered at 800 nm. The output from the laser system is splitted into two parts, the major part (90%) used to generate x-ray probe beam, and the other 10% used for the generation of the 266 nm pump pulse. A detailed description of the experimental system is included in ref 2. Briefly,

Static absorption spectrum obtained by excitation neutral Bz, ClBz, BrBz molecules from the core level to different unoccupied electronics orbitals by broadband soft x-ray pulses at the carbon K-edge region (high harmonics of a 1320 nm optical parametric amplifier output pumped by a Ti:sapphire laser). The spectrum recorded with ( $I_{gas}$ ) and without ( $I_{no\ gas}$ ) sample gas and calculated by:

$$A = -\log\left(\frac{I_{gas}}{I_{no\ gas}}\right)$$

Transient absorption spectrum,  $\Delta A$ , related to excitation the gas-phase Bz, ClBz, BrBz molecules with 266 nm which are then probed using temporally-delayed,

broadband, soft x-ray pulses at the carbon K-edge. The spectrum obtained by measuring the soft x-ray signal in the presence of the pump pulse ( $I_{on}$ ) at a given pump-probe time delay, relative to the x-ray signal in the absence of the pump pulse ( $I_{off}$ ) which blocked by electronic shutter.  $I_{on}$  signal consist of x-ray absorption from neutral and excited molecules where the absorption part of the neutral molecules we reduce with  $I_{off}$  signal by:

$$\Delta A = -\log\left(\frac{I_{on}}{I_{off}}\right)$$

The pump and probe beams focused and overlaps at a  $1^\circ$  crossing angle into a gas cell continuously flowing with a pressure of  $\sim 110, 8, 4$  Torr of Bz, ClBz, BrBz respectively. After the cell the probe pules spectrally dispersed by Hitachi grating (001-0660) onto an x-ray CCD camera (Princeton Instruments, PIXIS:XO 400B), where the entire broadband soft x-ray signal is measured at once as a function of the photon energy.

The absorbance with pump beam is of a mixture of both photoexcited and unexcited molecules; the concentration of each depends on the pump pulse parameters and absorption cross section of the sample at the pump wavelength used.

The UV excitation (5-35  $\mu\text{J}$ , 400  $\text{cm}^{-1}$  pulse full-width at half-maximum (FWHM) bandwidth,  $\sim 60$  fs pulse duration), can lead to two process; excitation from HOMO to LUMO, namely one photon  $\pi \rightarrow \pi^*$  transition (band origin transition from ground state to first excited state is 4.75, 4.593, 4.586 eV for Bz, ClBz, BrBz respectively) or ionization by (1+1) REMPI, namely promoted electron from HOMO ( $\pi$ ) to LUMO ( $\pi^*$ ) and then to infinity ( ionization energy from HOMO 9.243, 9.0722, 8.9976 eV for Bz,<sup>16</sup> ClBz,<sup>17</sup> BrBz<sup>18</sup> respectively ).

Due to system limitation of using wide range of UV beam power, the most effective way to change the relative amount of ions compare to the neutral one photon excited molecules was to work with 45 and 20 cm focal lenses which change the (1+1) REMPI efficiency very well, more detailed description mentioned in supplementary section.

The energy axis calibration is established using known absorption resonances near the  $L_{2,3}$ -edge of Ar between 240-250 eV and the carbon K-edge of allyl iodide and benzene around  $\sim 285$  eV, the FWHM value of the Gaussian function that characterizes the spectrometer resolution is found to be  $\sim 350$  meV.

## Results

The x-ray transition from the carbon core level of neutral molecules previously was measured. The main difference between Bz and BrBz spectra related to similar energy of core electronic level of all carbons in Bz compare to two different energetic core levels of carbons which bonded to hydrogen atom and to bromine atom. Consequently, it can be relatively convenient to start this study with benzene, and after resolving transient absorption spectrum of benzene it will be possible to continue with bromobenzene.

### Bz

Figure 2(a) shows a static spectrum of Bz at the carbon K-edge region. The first peak labeled as A, is well observed and known as  $1s(C) \rightarrow \pi^*(e_{2u})$  transition from previous works<sup>19,20,21,22,23</sup> the other peaks B, C and D were assignment as transitions to  $\sigma^*(C-C)$  and  $\sigma^*(C-H)$  with Rydberg characters<sup>24,23</sup> and as  $1s(C) \rightarrow \pi^*(b_{2g})$ <sup>20,22</sup> respectively, the energy of these transitions shown in table 1. Gaussian fit of  $1s(C) \rightarrow \pi^*(b_{2g})$  transition may be slightly shifted to the left side as it is possible to see that the fit is not perfect. It was suggested that vibronic transitions define peaks structure and amplitude as it can be seen in Fig 2(a) from the orange sticks.<sup>15</sup> It is worse to mention that it is not possible to observe so detailed structure with our system resolution (about 0.3 eV) and due to natural broadening, therefore we define peak position as a center of a fitted Gaussian.

Figure 1(b) shows a transient absorption spectrum of  $Bz^+$  with contribution from neutral excited Bz. The excitation and ionization accrues from the delocalized  $\pi$  orbitals. The most intense peak H in the transient absorption spectrum we assignment as  $1s(C) \rightarrow \pi^*(e_{2u})$  transition of  $Bz^+$ . This peak shifted by  $\sim 1.36$  eV to the lower energy compares to the same transition from the ground state (in the static spectrum). This behavior can be observed in ClBz and BrBz molecules too. From power depends study (and different focusing conditions) we conclude that this peak related to cation. Since the molecule has one electron less in the valance state and consequently, the repulsive force on the electrons in the core level expected to be smaller, it leads to lower transition energy from the core level to higher excited levels of  $Bz^+$ . This tentative explanation can rationalize this shift. Another well-defined peak J, observed

4.2 eV higher, very similar to the energetic distance between  $\pi^*(e_{2u})$  and  $\pi^*(b_{2g})$  in neutral Bz (assigned in the static spectrum), and therefore we assign this peak as  $1s(C) \rightarrow \pi^*(b_{2g})$ . (For simplicity, I note the symmetry of the states according to the symmetry of the ground state as in static spectrum)

By taking one electron from  $\pi(e_{1g})$  orbital which energetically located about 4.75 eV from  $\pi^*(e_{2u})$  we open a new possible transition. This transition observed clearly as peak E at 279.25 eV which is shifted from  $1s(C) \rightarrow \pi^*(e_{2u})$  transition by 4.8 eV. From above mentioned, we assign this transition as  $1s \rightarrow \pi$  of  $Bz^+$ .

Peak G observed at 281.27 eV and peak F observed as a dominant shoulder at 280.3 eV. Due to the observed red shifted (as mentioned before) transitions to  $\pi^*$  orbital of  $Bz^+$  compare to neutral Bz, we expect to see similar shift to  $1s \rightarrow \pi$  transition, and therefore peak F can be assign as  $1s \rightarrow \pi$  transition of Bz (about 5 eV from peak A and 1.1 eV from peak E). While peak G can be assigned as  $1s \rightarrow \pi$  transition of the elongated  $Bz^+$  form where peak E related to compressed form. From mentioned above, the energetic splitting between two  $Bz^+$  forms more significant in  $1s(C) \rightarrow \pi$  transitions compare to  $1s(C) \rightarrow \pi^*$  where the splitting not observed from the spectrum. To rationalize this observation we can propose tentative assumption that the major impact of J-T effect is on the  $\pi$  orbitals which are closer to the nucleus and therefore the correlation between these orbitals with benzene ring structure (with nucleus) is larger compare to  $\pi^*$  orbital. In this case, the degenerated  $\pi^*$  orbitals not expected to have very different structure and consequently significant splitting not observed.

It is worth to note, the influence of removing one electron from a degenerate  $\pi(e_{1g})$  orbital during the ionization process expected to be similar on the all six carbons because the  $\pi$  orbitals are delocalized on the benzene ring, therefore the expectation to see two different  $1s \rightarrow \pi$  transitions corresponded to two new structure of  $Bz^+$  with different electronic distribution due to J-T effect. The geometrical change of the benzene ring can lead to energetic shift of the core level of different carbons, but this shift is probably smaller than our resolution (not observed in static spectrum of ClBz or BrBz).

Peak I may related to  $1s \rightarrow \sigma^*$  transition of  $Bz^+$  or excited Bz. In addition possible explanation of this peak is transition to another  $\pi^*$  orbital (there are three  $\pi^*$ ),

this transition forbidden in the ground state geometry but after ionization in addition to impact from vibronic coupling this transition can be bright.

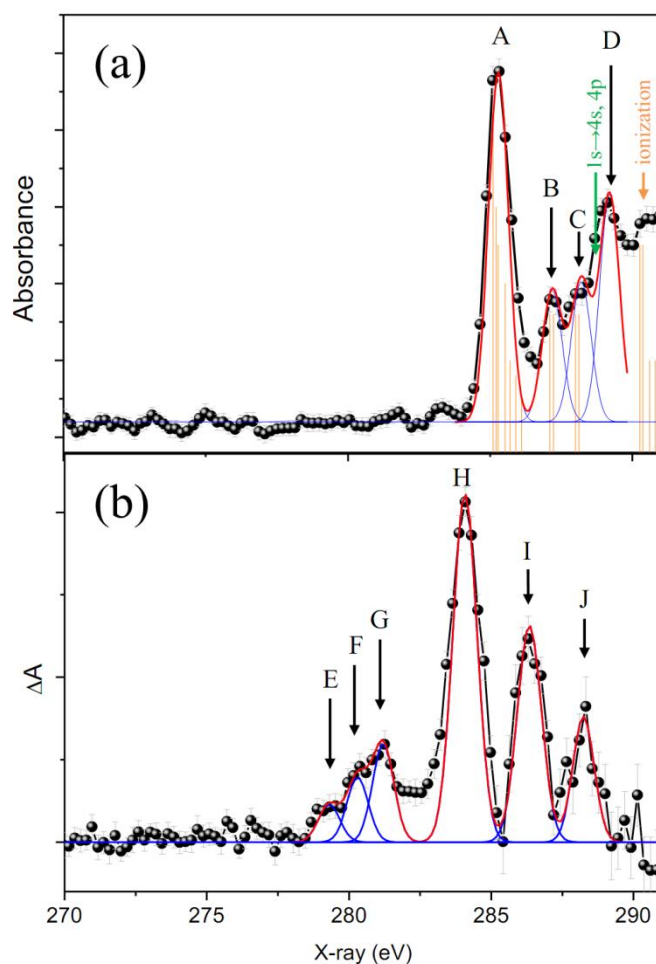


**Figure 2.** Static and transient absorption spectrum of Bz at carbon K-edge. (a) The black line connecting the data points (black circles) corresponds to experimental static spectrum, where blue lines are Gaussian fits to the peaks (FWHM 0.824 eV), the red solid line is the summation of all the fitted Gaussians, and orange sticks corresponds to transitions to vibrational states taken from ref 22, 15 (b) The black line connecting the data points correspond to experimental transient absorption spectrum ( $\Delta A$ ), blue lines are Gaussian fits (FWHM 0.88 eV for E, F, G and 1eV for H, I, J) and red solid line is summation of all fitted Gaussians. The assign of Peaks A-J is shown in Table 1.



**Table 1.** Assignments of observed Peaks of Bz.

Peak	Energy (eV)	Assignment	known energy (eV)
<b>Static absorption spectrum</b>			
A	285.30	$1s(C) \rightarrow \pi^*(e_{2u})$	285.20, <sup>19</sup> 285.11 <sup>23</sup> , 285.1 <sup>25</sup>
B	287.18	$1s(C) \rightarrow 3S, \sigma^*(C-C)$	287.50, <sup>19</sup> 287.17 <sup>23</sup> , 287.2 <sup>25</sup>
C	288.20	$1s(C) \rightarrow 3p, \sigma^*(C-H)$	288.00, <sup>19</sup> 287.92 <sup>23</sup> , 287.9 <sup>25</sup>
D	289.20	$1s(C) \rightarrow \pi^*(b_{2g})$	288.90, 289.1 <sup>25</sup>
<b>Transient absorption spectrum</b>			
E	279.20	$1s \rightarrow \pi (Bz^+)$ compressed form	-
F	280.30	$1s(C) \rightarrow \pi (Bz)$	-
G	281.27	$1s \rightarrow \pi (Bz^+)$ elongated form	-
H	284.10	$1s(C) \rightarrow \pi^*(e_{2u}) (Bz^+)$	-
I	286.28	$1s(C) \rightarrow \pi^*(e_{2u} [a_2]) (Bz^+)?$ $1s(C) \rightarrow \sigma^*(C-C)?$	-
J	288.30	$1s(C) \rightarrow \pi^*(b_{2g}) (Bz^+)$	-

**BrBz**

Figure 3(a) shows a static spectrum of BrBz in the carbon K-edge region. The first peak labeled as A, is well observed and known as  $1s(C) \rightarrow \pi^*(2b_1)$  transition,<sup>19</sup> very similarly to Bz. Peak B labeled as  $1s(C_1) \rightarrow \pi^*(2b_1)$ , where 1s orbital of  $C_1$  carbon blue shifted compare to the other carbons due to higher electron density from Cl atom, this shift corresponds to 1 eV while the  $\pi^*$  orbital is very same for both transition and almost unaffected by halogen atom. (This assumed due to the same difference between transition to  $\pi^*$  compare to binding energy related to 1s of C and  $C_1$  as shown in ref 19) peak C and D we assign as  $1s(C) \rightarrow \sigma^*$  with possible 5s characters, and  $1s(C_1) \rightarrow \sigma^*$  5s transitions respectively, very similar to the assigned spectrum of FBz.<sup>20</sup> Another possibility is to include  $1s(C) \rightarrow 5p, \sigma^*$  in this region as was done in ref 19 but it is impossible to observe any clear transition. Peaks E and F assigned as  $1s(C) \rightarrow \pi^*(1b_1)$  and  $1s(C) \rightarrow \pi^*(1b_1)$  based on FBz assignment.<sup>20</sup> the center of the fitted Gaussians of these transitions shown in table 2. We assume that the peak width depends very much on vibrational transition as in Bz and influenced from a possible small shift in the 1s levels of the five carbons caused by bromine atom.

Figure 3(b) shows a transient absorption spectrum of  $BrBz^+$  and Figure 2(c) shows a transient absorption spectrum of  $BrBz^+$  with some contribution from neutral excited BrBz. The difference in experiment conditions of 2(b) spectra compare to 2(c) is the focusing conditions of the UV beam. for 2(b), 20 cm f.l was used, in this condition the second photon is strongly saturated (reducing the power from ~30 to

$\sim 10 \mu\text{J}$  still provide almost linear ratio with slope close to 1 for  $\log(\text{power})/\log(\text{signal})$ , for lower UV power the signal disappear. due to small interaction region that we had between UV and X-ray beam) and therefore the major part related to  $\text{BrBz}^+$ , spectrum 2(c) was measured with 45 cm f.l, in these conditions we can observe contribution from the excited neutral  $\text{BrBz}$ .

The most intense peak H in the transient absorption spectrum we assignment as  $1s(\text{C}) \rightarrow \pi^*(2b_1)$  transition of  $\text{BrBz}^+$ . This peak shifted by  $\sim 1.3 \text{ eV}$  (with relatively big error due to the double form of the peak) to lower energy compare to the same transition of neutral  $\text{BrBz}$  without UV excitation, very similarly to  $\text{Bz}^+$ . Next very well observed peak in Figure 3(b) is K, it assigned as  $1s(\text{C}) \rightarrow \pi^*(1b_1)$  of  $\text{BrBz}^+$  with very similar consideration as it was assigned in  $\text{Bz}^+$ , energetic distance between peak H and K is very similar to A and E. In addition, it is possible to observe a very weak peak I.

In figure 3(c), transitions of  $\text{BrBz}^+$  are observed, peaks H and K. Moreover, due to significant amount of neutral excited molecules we observe several changes compare to figure 3(b). Peaks G, J and strong depletion (marks as A because it related to subtraction of peak A). As for the depletion, It lead us to conclude that in position of peak A,  $1s(\text{C}) \rightarrow \pi^*(2b_1)$  transition (assumed the position does not change a lot) of the neutral excited molecule has smaller or similar cross section compare to not excited molecule. In addition, more obvious conclusion is that in figure 3(b) the depletion not observed due to additional absorption band related to  $\text{BrBz}^+$ .

In figure 3(c), peak J is assigned as  $1s(\text{C}_1) \rightarrow \pi$  transition due to  $\pi \rightarrow \pi^*$  excitation with UV. The energetic distance from  $\pi^*$  expected to be about 4.6 eV (in frozen geometry) therefore we assigned it as transition from  $\text{C}_1$  (about 4.3 eV from peak B, but as can be seen from the spectrum the position of the fitted Gaussian can slightly blue shifted). On the left side of this peak it can be observe a shoulder, (about 0.7 eV shifted) which can be assigned as  $1s(\text{C}) \rightarrow \pi$  transition. From this picture we see a dramatic change in excitation probability from C compare to  $\text{C}_1$  due to UV excitation. (in static spectrum the major transition occurs from C atoms, carbons bonded with hydrogen atoms) From this consideration we assign peak J as  $1s(\text{C}_1) \rightarrow \pi^*$ , (the position of this peak very similar compare to peak B in figure 3(a) )

while  $1s(C) \rightarrow \pi^*$  transition became weaker and therefore we observe significant negative peak A.

By adding back relative contribution of static spectrum we can observe peak J in figure 4(a) but as expected with much smaller amplitude compare to the two main transitions. From this spectrum we can observe peak I. we assign this peak as  $1s(C_1) \rightarrow \pi^*$  transition of  $BrBz^+$  due to energetic difference between  $1s$  of C atoms and  $C_1$  atom. As well, peak J grow up in figure 4(b) while peak G remains without change because it's shifted compare to the static spectrum.

In figure 3(b) and 3(c) peaks K and H contain two parts separated by about 0.6 eV, 283.95 and 284.54 eV, 287.70 and 288.30 eV. This structure can be related to compressed and elongated forms which corresponded to  $X^2B_1$  and  $A^2A_2$  states of the cation respectively. This assumption lead as to predict that at very short time delay between UV and x-ray beam we expect to observe peaks K and H with only one part, and observation of the second part of the peaks structure related to time where the molecule pass through predicted conical intersection which lead to the elongated forms of the benzene ring. (Conical intersection shown in figure 1)

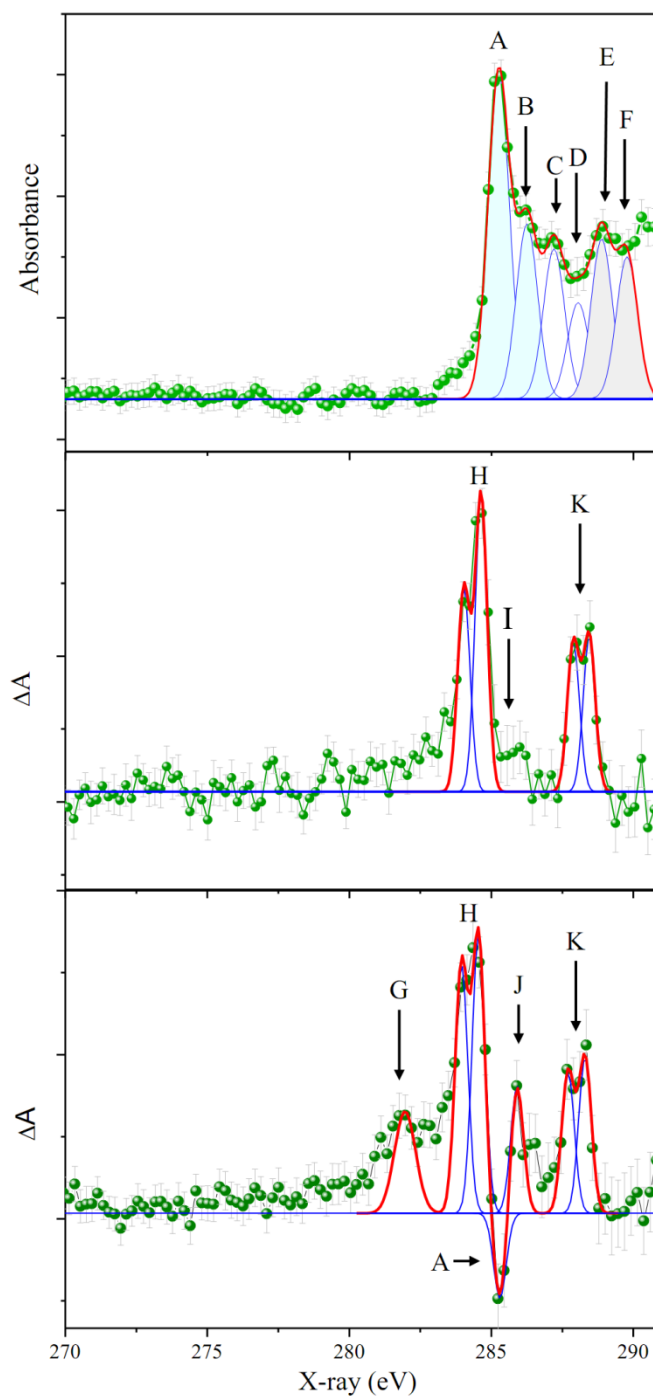


**Figure 3.** Static and transient absorption spectrum of BrBz at carbon K-edge. (a) The green line connecting the data points (green circles) corresponds to experimental static spectrum, where blue lines are Gaussian fits to the peaks (FWHM 0.824 eV), the red solid line is the summation of all the fitted Gaussians. (b) The green line connecting the data points correspond to experimental transient absorption spectrum, blue lines are Gaussian fits to the peaks (FWHM 0.94 eV) and red solid is summation of all fitted Gaussians. Peaks A-K are assigned in Table 2.

**Table 2.** Assignments of Observed Peaks of BrBz.

Peak	Energy (eV)	Assignment	known energy (eV)
<b>Static absorption spectrum</b>			
A	285.25	$1s(C) \rightarrow \pi^*(2b_1)$	285.1
B	286.25	$1s(C_1) \rightarrow \pi^*(2b_1)$	286
C	287.20	$1s(C) \rightarrow 5S, \sigma^*$	287
D	288.05	$1s(C_1) \rightarrow 5S, \sigma^*$	288
E	288.88	$1s(C) \rightarrow \pi^*(1b_1)$	289
F	289.77	$1s(C_1) \rightarrow \pi^*(1b_1)$	290.2
<b>Transient absorption spectrum</b>			
G	281.95	$1s(C_1) \rightarrow \pi (Bz)$	-
H	283.95	$1s(C) \rightarrow \pi^*(2b_1) (Bz^+)$	-
	284.54	$1s(C) \rightarrow \pi^*(2b_1) (Bz^+)$	
I	285.3	$1s(C) \rightarrow \pi^*(2b_1) (Bz)$	-
J	285.91	$1s(C_1) \rightarrow \pi^*(2b_1) (Bz)$	-
K	287.70	$1s(C) \rightarrow \pi^*(1b_1) (Bz^+)$	-
	288.30	$1s(C) \rightarrow \pi^*(1b_1) (Bz^+)$	

The known energy taken from ref 19.

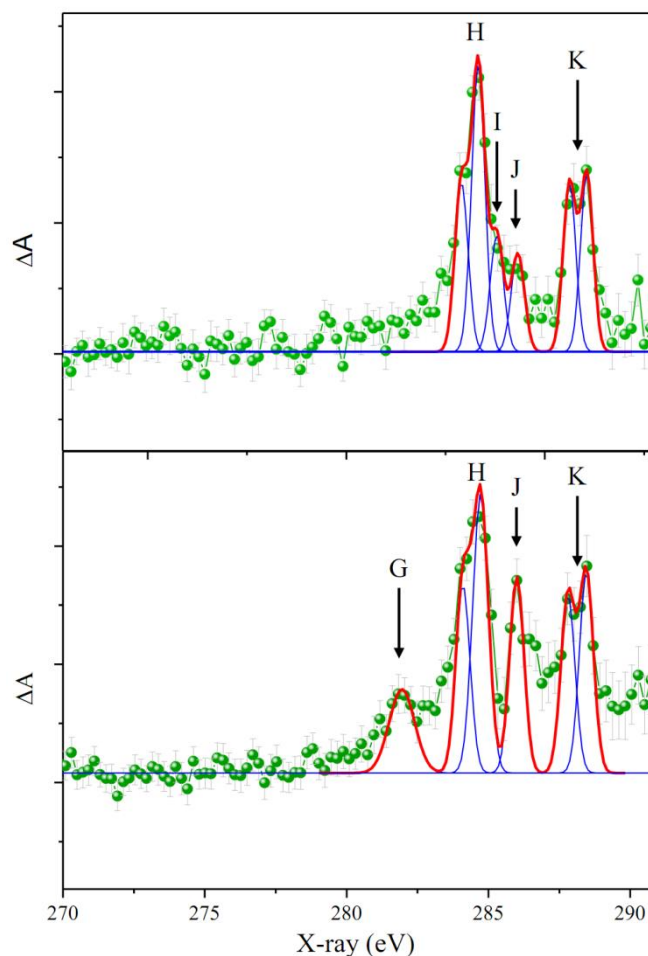


**Figure 4.** Transient absorption spectrum of BrBz at carbon K-edge converted to pure spectra with UV photoexcited neutral or ionized molecules by adding back a scaled static spectrum without UV excitation based on the estimated percentage of the

molecules in the interaction region that are photoexcited. (a) The green line connecting the data points (green circles) corresponds to experimental static spectrum after adding back 10% of static spectrum without UV excitation, by adding back 20% does not change significantly the spectrum except higher amplitude of peak I and J and small broadened of peak H on the right side. blue lines are Gaussian fits to the peaks (FWHM 0.824 eV), the red solid line is the summation of all the fitted Gaussians. (b) The green line connecting the data points of experimental transient absorption spectrum after adding back 15% of static spectrum to aliminate the depletion band, blue lines are Gaussian fits to the peaks (FWHM 0.94 eV) and red solid is summation of all fitted Gaussians.

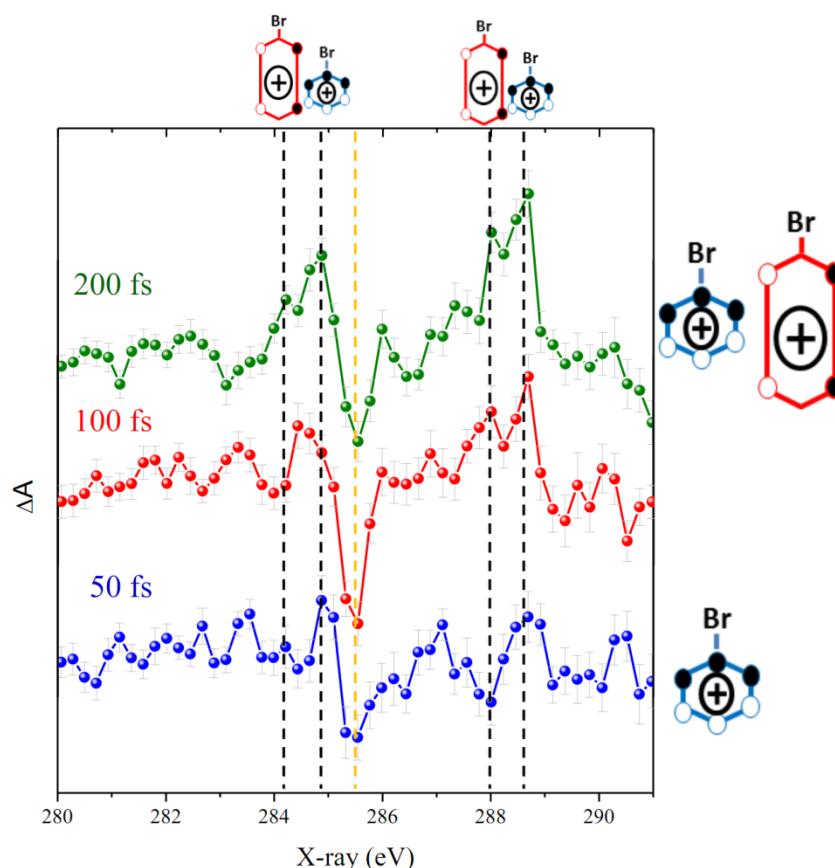


**Figure 5.** . Experimental soft x-ray transient absorption spectrum,  $\Delta A$  measured at different time delay between the UV (pump) and X-ray (probe) beams. The blue line corresponds to about 50 fs time delay, where the major contribution to  $1s(C) \rightarrow \pi^*(2b1)$  and  $1s(C) \rightarrow \pi^*(1b1)$  transitions come from compressed  $BrBz^+$  form (dashed line). Red line corresponds to 100 fs, and green line corresponding to 200 fs where both compressed and longitude forms contribute to the  $1s(C) \rightarrow \pi^*(2b1)$  and  $1s(C) \rightarrow \pi^*(1b1)$  transitions .

## conclusions

- By taking one electron from  $\pi$  orbital (HOMO) we open a possibility to promote one electron from the core level to this orbital. This transition we can observe very clearly in excited Bz, BrBz and  $\text{Bz}^+$ . While the cross section of this transition much higher for neutral excited molecule compare to cation.
- It is possible to observe J-T splitting in  $\text{Bz}^+$ , by transitions from the core level to  $\pi$  orbitals related to two different forms, while transition to  $\pi^*$  is less sensitive to the splitting.
- In BrBz it is possible to observe two different electronic states (compressed and elongated form) from transition to  $\pi^*$ . while transition to  $\pi$  not observed.
- In excited BrBz the transition from  $\text{C}_1$  atom (carbon bonded to bromine atom) to  $\pi$  and  $\pi^*$  orbitals is significantly higher compare to transition cross section from C atoms (carbons bonded to hydrogen) while transitions to  $\pi^*$  without UV favorite from C.
- The passage through predicted CI between  $\text{X}^2\text{B}_1$  and  $\text{A}^2\text{A}_2$  was observed, this passage happens in less than 100 fs.???

## UV power depend study and focusing conditions

From previews works it is known that 266 nm beam can easily produce (1+1) REMPI, for example, even with 0.5  $\mu\text{J}$ , ~100 fs pulse the ionization of ClBz and especially BrBz play a significant role compare to the one photon excited of neutral molecules.<sup>26</sup> In our case, the power depend study with 20 cm f.l. shows almost linear relation between the signal and UV power, it is indicate that the second photon of the ionization process close to saturation. Despite very efficient REMPI process at 10  $\mu\text{J}$  it is possible to see a small contribution of neutral molecules, see peak G in figure 6. At 5  $\mu\text{J}$  the signal is already very low and it is very hard to observe a clear spectrum and therefore it was impossible to lower the UV power. By switching the f.l. to 45 cm, the interaction region with x-ray beam expected to enlarge while the probability for ionization expected to decrease. The observed peak in predicted position of  $1\text{S}(\text{C}) \rightarrow \pi$  transition of neutral BrBz indicated on a small amount of neutral molecules. For Bz, the neutral excited molecules are observed with 20 cm f.l. as well.

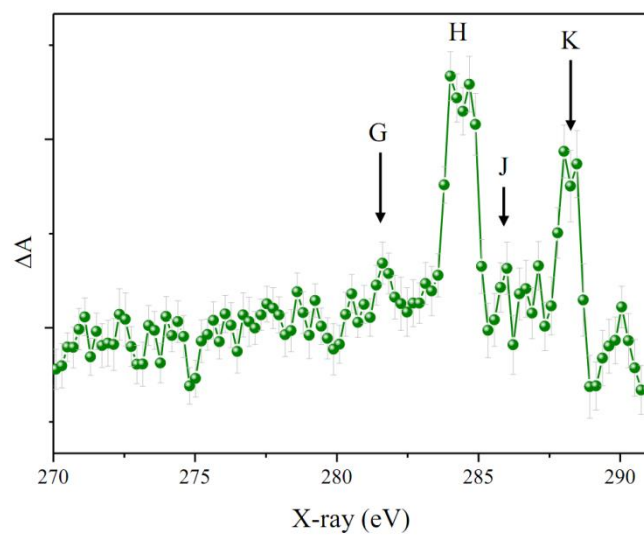


**Figure 6.** Transient absorption spectrum of BrBz at carbon K-edge pumped by UV beam intensity of  $\sim 10 \mu\text{J}$ .



- 
- <sup>1</sup> H. A. Jahn and E. Teller, *Proc. R. Soc. London Ser. A*, 161, 220 (1937).
- <sup>2</sup> A. R. Attar, A. Bhattacharjee, C. D. Pemmaraju, K. Schnorr, K. D. Closser, D. Prendergast, S. R. Leone, *Science*, 356, 54-59 (2017)
- <sup>3</sup> A. Bhattacharjee, C. Das Pemmaraju, K. Schnorr, A. R. Attar, S. R. Leone, *J. Am. Chem. Soc.* 139 (46), 16576–16583 (2017).
- <sup>4</sup> A. Bhattacharjee, K. Schnorr, S. Oesterling, Z. Yang, T. Xue, R. de Vivie-Riedle, S. R. Leone. *J. Am. Chem. Soc.* (2018).
- <sup>5</sup> R. Lindner, K. Muller-Dethlefs, E. Wedum, K. Haber, and E. R. Grant, *Science*. 271, 1698 (1996).
- <sup>6</sup> K. Raghavachari, R. C. Haddon, T. A. Miller, and V. E. Bondybey, *J. Chem. Phys.* 79, 1387 - 1395 (1983).
- <sup>7</sup> H. Tachikawa, *J. Phys. Chem. A*, 122, 4121 - 4129 (2018).
- <sup>8</sup> M.H. Palmer, T. Ridley, S.V. Hoffmann, N. C. Jones, M. Coreno, M.d. Simone, C. Grazioli, M. Biczysko, A. Baiardi, *J. Chem. Phys.* 142, 134302 (2015). **IBz**
- <sup>9</sup> M.H. Palmer, T. Ridley, S.V. Hoffmann, N. C. Jones, M. Coreno, M.d. Simone, C. Grazioli, T. Zhang, M. Biczysko, A. Baiardi, K.A. Peterson, *J. Chem. Phys.* 144, 124302 (2016). **CIBz**
- <sup>10</sup> M. H. Palmer, T. Ridley, S. V. Hoffmann, N. C. Jones, M. Coreno, M. de Simone, C. Grazioli, T. Zhang, M. Biczysko, A. Baiardi, and K. Peterson, *J. Chem. Phys.* 143, 164303 (2015). **BrBz**
- <sup>11</sup> M.H. Palmer, T. Ridley, S.V. Hoffmann, N. C. Jones, M. Coreno, M.d. Simone, C. Grazioli, T. Zhang, M. Biczysko, A. Baiardi, and K.A. Peterson, *J. Chem. Phys.* 144, 204305 (2016). **FBz**
- <sup>12</sup> I. Bâldea, J. Franz, P. Szalay, and H. Köppel, *Chem. Phys.* 329, 65 (2006).
- <sup>13</sup> E. Gindensperger, I. Bâldea, P. G. Szalay, and H. Köppel, *Chem. Phys.* 338, 207 (2007).
- <sup>14</sup> S. Sardar, P. Puzari, and S. Adhikari, *Chem. Phys. Lett.* 496, 341 (2010).
- <sup>15</sup> V. Myrseth, K. J. Børve, K. Wiesner, M. Baßler, S. Svensson and L. J. Sæthre, *Phys. Chem. Chem. Phys.*, 4, 5937–5943 (2002).
- <sup>16</sup> P. Baltzer, L. Karlsson, B. Wannberg, G. Ohrwall, D. M. P. Holland, M. A. MacDonald, M. A. Hayes, and W. von Niessen, *Chem. Phys.* 224, 95 (1997).
- <sup>17</sup> G. Lembach, B. Brutschy, *Chem, Phys, Lett*, 273, 421-428 (1997).
- <sup>18</sup> C. H. Kwon, H. L. Kim, and M. S. Kim, *J. Chem. Phys.* 116, 10361 (2002).
- <sup>19</sup> A.P.Hitchcock, M.Pocock, C.E.Brion, M.S.Banna, D.C.Frost, C.A.McDowell, and B.Wallbank, *Journal of Electron Spectroscopy and Related Phenomena*, 13, 345 - 360 (1978).
- <sup>20</sup> W. H. E. Schwarz, T. C. Chang, U. Seeger, and K. H. Hwang, *Chem. Phys.* 117, 73 -89 (1987).
- <sup>21</sup> Y. Ma, F. Sette, G. Meigs, S. Modesti, and C. T. Chen, *Phys. rev. let.* 19, 2044 - 2047 (1989).
- <sup>22</sup> E. E. Rennie, B. Kempgens, H. M. Köppe, U. Hergenhahn, J. Feldhaus, B. S. Itchkawitz, A. L. D. Kilcoyne, A. Kivimäki, K. Maier, M. N. Piancastelli, M. Polcik, A. Rüdell, and A. M. Bradshaw *J. Chem. Phys.* 113 (2000)
- <sup>23</sup> R. Püttner, C. Kolczewski, M. Martins, A.S. Schlachter, G. Snell, M. Sant’Anna, J. Viefhaus, K. Hermann, G. Kaindle, *Chem. Phys. Lett.* 393, 361 - 366 (2004)

- 
- <sup>24</sup> D. Menzel, G. Røcker, H.-P. Steinrück, D. Coulman, P.A. Heimann, W. Huber, P. Zebisch, D.R. Lloyd, **J. Chem. Phys.** 96 1724 - 1733 (1992).
- <sup>25</sup> C. Kolczewski, R. Püttner, M. Martins, A. S. Schlachter, G. Snell, M. M. Sant'Anna, K. Hermann, and G. Kaindl, **J. Chem. Phys.** 124, 034302 (2006)
- <sup>26</sup> M. Kadi, J. Davidsson, A.N. Tarnovsky, M. Rasmusson, E. Åkesson. **Chem Phys Lett** **350**, 93-98 (2001).